A 2D/1D Method for Consistent Burnup Parametrization of Cross Sections in SFR Fuel Depletion Calculations

B. Faure, P. Archier, L. Buiron

PHYTRA4 - The Fourth International Conference on Physics and Technology of Reactors and Applications.
Marrakech, Morocco, September 17-19, 2018, on CD-ROM, GMTR, Rabat, Morocco (2018)

A 2D/1D METHOD FOR CONSISTENT BURNUP PARAMETRIZATION OF CROSS SECTIONS IN SFR FUEL DEPLETION CALCULATIONS

Bastien Faure, Pascal Archier and Laurent Buiron
CEA, DEN, DER, SPRC
Cadarache, F-13108, Saint-Paul-lez-Durance, France
bastien.faure@cea.fr

ABSTRACT

The accuracy of neutronic calculations in reactor physics is determined by the quality of the averaged cross sections used to solve the Boltzmann transport equation. As the reactor burns its fuel, a change occurs in the neutronic properties of the media so the averaged cross sections become time-dependent. Several transport calculations are therefore required at the cross section generation stage to perform a burnup (or fluence) parametrization of the data. This paper proposes to use the now well known 2D/1D method to perform this parametrization. The idea of such a strategy is to avoid computationally expensive 3D simulations while overcoming the drawbacks of standard 2D models. The algorithm is applied to produce time-dependent effective cross sections for a SFR fuel assembly with CFV design. The fuel depletion analysis is then conducted in a "core environment" and results are compared to independent Monte Carlo simulations. Good performances are found both for the evolution of the spatial distribution of isotopic concentrations and the assembly reactivity loss.

Key Words: Fuel depletion, Neutron Transport, 2D/1D Method

1. INTRODUCTION

The neutronic calculation of a nuclear reactor core consists in solving a Boltzmann transport equation whose solution is the neutron flux. Its knowledge gives access to several quantities of interest such as the power map, the multiplication factor or the evolution of the fuel inventory.

Unfortunately, time dependent three-dimensional fine calculations are still out of range of even the most powerful super-computers. When the reactor is in normal operating conditions though, the change in the flux shape is slow compared to the evolution of the fuel composition. Is is then licit to use an adiabatic approximation which enables transforming the time dependent Boltzmann transport equation into a succession of steady state problems [1]. Between two time steps, isotopic compositions are updated by solving a set of Bateman equations [2].

Even so, solutions of steady state problems often require long hours of calculation over large-scale parallel computers. For practical applications, full core calculations are therefore performed over both spatial and energy coarse meshes. Thus, they rely on homogenized multigroup *effective cross sections* which are flux-weighted average of the input fine group nuclear data.

As the reactor operates, the fuel depletion induces a change in the neutronic properties of the media and consequently in the flux spectrum and spatial distribution. As a result, effective microscopic cross sections become time-dependent. The burnup parametrization of cross sections provides an

efficient way to account for that change. It also allows to manage the core reloading strategy (i.e. the fact that each fuel assembly has his own local burning rate).

Traditionally, the burnup parametrization of cross sections relies on two-dimensional assembly calculations for which the flux level is normalized to the averaged reactor power. This strategy however fails when the flux presents sharp axial gradients. It is the case in modern Sodium Fast Reactor (SFR) designs that tend to present axial heterogeneities such as fertile blankets and even sodium plenums.

This paper proposes to take into account the three-dimensional geometry of a fuel assembly to perform the burnup parametrization of cross sections. In order to avoid expensive 3D flux calculations, a 2D/1D approximation - inspired of Cho's *fusion method* [3] - is carried out to solve the neutron transport equation. The 1D solution is used both to supply axial leakage for 2D calculations and to normalize the flux to the true assembly power. Time-dependent consistent effective cross sections are therefore produced for the entire fuel assembly including fertile blankets, structures and shields.

The organization of this paper is as follows. Section 2 presents how the 2D/1D method can be used to produce time-dependent effective cross sections for SFR applications while Section 3 is devoted to numerical results obtained with the APOLLO3® code [4]. The benchmark chosen for application is a reflected 3D fuel assembly representative of the CFV (*coeur a faible vidange* or low sodium void effect core) which is under study at CEA in France as part of the ASTRID project [5].

2. BURNUP PARAMETRIZATION OF CROSS SECTIONS WITH THE 2D/1D METHOD

2.1. The Transport Equation

In the scope of fuel depletion calculations, the time-dependent Boltzmann neutron transport equation is often replaced by a system involving Bateman equations and the steady state form of the transport equation. While the former rules the evolution of materials under irradiation, the latter handles the level and spatial distribution of the nuclear reaction rates. This system reads:

$$\begin{cases} (\boldsymbol{\Omega} \cdot \boldsymbol{\nabla} + \Sigma)\, \psi = q & \text{(1a)} \\ \dfrac{d\boldsymbol{N}}{dt} = \mathbb{A}(\boldsymbol{\lambda}, \boldsymbol{\tau})\boldsymbol{N} & \text{(1b)} \end{cases}$$

where Eq. (1a) is the steady state Boltzmann transport equation and Eq. (1b) is the matrix form of the Bateman equations. The macroscopic total cross section $\Sigma = \sum_k N_k(t)\sigma$ is a sum over all the isotopes of their concentration N_k times their microscopic total cross section σ. q is the source term that includes contributions from fission and scattering and ψ is the neutron flux. $\boldsymbol{N}$ is the vector of isotopic concentrations and $\mathbb{A}$ the evolution matrix that depends on decay constants $\boldsymbol{\lambda}$ and reaction rates $\boldsymbol{\tau}$.

The solution of the above system is obtained by successively solving Eq. (1a) to get fluxes and reaction rates and Eq. (1b) to update the isotopic concentrations.

2.2. The 2D/1D Algorithm for Cross Section Generation

This section focuses on the resolution of Eq. (1a). It presents how the 2D/1D method can be used to avoid full 3D calculations when producing effective cross sections. The ideas of section 2.2.1 have already been exposed in our previous work [6] but they are recalled here for the sake of clarity.

2.2.1. General Equations

In the scope of cross section generation, the geometrical domain over which Eqs. (1a) and (1b) need to be solved is typically a fuel assembly with reflective radial boundary conditions. If axial heterogeneities are present, the entire (3D) geometry should be considered.

But if cross sections are axially invariant in a domain $[z_i-; z_i+]$ and if a flat shape is assumed for axial leakage, which is not so far from reality in SFR, it is shown in reference [6] that the successive integration of Eqs. (1a) in the axial and radial directions yields the following set of 2D/1D equations:

$$\begin{cases} \left(\mathbf{\Omega} \cdot \boldsymbol{\nabla}_{xy} + \Sigma\right) \psi_i = q_i - L_i & \text{(2a)} \\ \left(\mu \dfrac{\partial}{\partial z} + \Sigma_r\right) \psi_r = q_r & \text{(2b)} \end{cases}$$

where ψ_i, q_i (resp. ψ_r, q_r) are the axially (resp. radially) integrated flux and source and Σ_r is the radially homogenized total cross section. L_i is the axial leakage:

$$L_i = \frac{\mu}{A_{xy}} \psi_r|_{z_i-}^{z_i+} \tag{3}$$

with μ the polar cosine and $A_{xy} = \int_{D_r} dxdy$ the radial area of the pattern. The fact that radial leakage do not appear in Eq. (2b) is a direct consequence of the reflective radial boundary condition.

The solution of the above system is obtained by iteratively solving Eq. (2a) in each 2D layer of the fuel assembly (with index i) using axial leakage given by Eq. (3) and retrieved from Eq. (2b). Iterations are required because Σ_r is homogenized with fluxes ψ_i:

$$\Sigma_{r,i} = \frac{< \Sigma\psi_i >_{D_r}}{< \psi_i >_{D_r}}. \tag{4}$$

2.2.2. Transverse Leakage Splitting

In the iterative resolution of the 2D/1D equations, instabilities may arise when the right hand side of Eq. (2a) is negative. In our previous work, the problem was avoided by neglecting those sources that have a negative isotropic component i.e. when $0 < L_{i,00} = \int_{4\pi} d^2\Omega\, L_i$.

In this paper however, another solution inspired by the work of the MPACT development team [7] is proposed: the "'transverse leakage splitting technique" (TLS). It consists in replacing negative leakage by an additional contribution in the macroscopic total cross section. In that case, whenever

the isotropic component of the axial leakage is negative, Eq. (2a) is replaced by:

$$\begin{cases} \left(\boldsymbol{\Omega}\cdot\boldsymbol{\nabla}_{xy}+\widetilde{\Sigma}\right)\psi_i = q_i - \widetilde{L}_i & \text{(5a)} \\ \widetilde{\Sigma} = \Sigma + \dfrac{L_{i,00}}{\psi_{i,00}} & \text{(5b)} \\ \widetilde{L}_i = L_i - \psi_i \dfrac{L_{i,00}}{\psi_{i,00}} & \text{(5c)} \end{cases}$$

where $\psi_{i,00} = \int_{4\pi} d^2\Omega\ \psi_i$. It can be seen that the system of Eqs. (5a), (5b) and (5c) is fully consistent with Eq. (2b) and that it still defines a transport equation over an isotropic medium.

With those definitions, the modified leakage source $\widetilde{L}_i$ has null isotropic component so most instabilities are avoided. The high angular orders of $\widetilde{L}_i$ can still pose some problems but our experience showed that the method is stable in nearly every case. The only exception we found so far is the case of "over-critical" planes (i.e. planes for which the number of neutrons produced by fission exceeds the number of neutrons being absorbed). The way the issue is dealt with is explained in reference [6].

For practical application of the TLS in the APOLLO3® code, it is worth mentioning that flux ψ_i is replaced by its mean value in the expressions of the modified cross section Eq. (5b) and source Eq. (5c) i.e. $\psi_i \approx \frac{1}{A_{xy}}\int_{D_r} dxdy\ \psi_i = \frac{1}{A_{xy}}\int_{z_i-}^{z_i+} dz\ \psi_r$. This allows to compute the correction term directly from the solution of Eq. (2b).

2.2.3. Cross Section Collapsing

When the system is converged, cross sections are homogenized in each 2D layer (index i). A summation is also performed over the energy groups in order to reduce their number to a few tens maximum (33 in this work). The averaged cross sections are stored in a library for future core calculations.

In this paper, the (angular) "flux moments" collapsing technique proposed in reference [8] is used. It is preferred to the standard flux-volume weighting formulas because these do not preserve the angular information (flux anisotropy in the calculation domain). On the other hand, the flux moments collapsing technique uses the angular moments of the flux to weight cross sections in a consistent way.

This theory is relevant in the scope of the 2D/1D equations since angle dependent leakage are used in Eq. (2a).

2.3. Burnup Parametrization

The 2D/1D framework provides a natural way to perform the coupling of the Boltzmann and Bateman equations.

Starting from a fresh fuel assembly, Eqs. (2a) and (2b) are first solved (with TLS eventually). The flux is then normalized to the assembly power and normalized reaction rates are supplied

to Eq. (1b). Once the Bateman equations are solved, the vector of isotopic concentrations $\boldsymbol{N}$ is updated and the process is repeated. At each step, effective cross sections are stored in a parametric library referenced by the local burnup (or fluence for structures and shields).

Time-dependent fully consistent cross sections are thus produced for the entire fuel assembly. This iterative procedure is summarized in Figure 1.

The advantage of this strategy is that it uses the local assembly power, which is usually a realistic (and even measurable) parameter of the core, whereas standard 2D calculations use an average value of the power to normalize the flux. In addition, it consistently takes into account any change in the axial flux shape which can be significant in heterogeneous core designs.

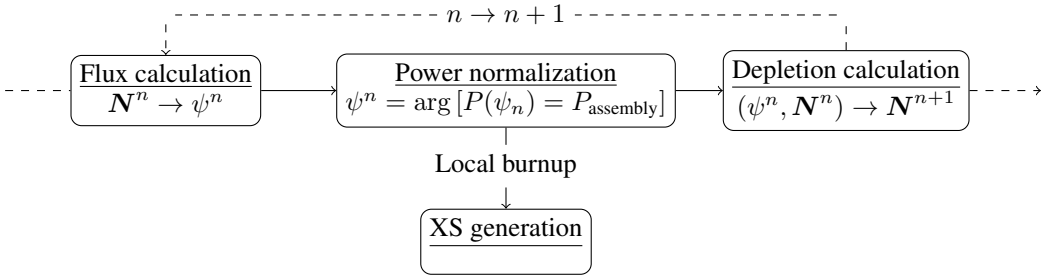

Figure 1. Fuel depletion calculations

Finally, it should be said that solving Eqs. (2a) and (2b) at each time step might be time consuming especially for those planes that do not contain depleting materials (structures, shields...). To avoid doing so, our implementation of the algorithm allows to selectively choose planes for which Eq. (2a) is to be solved at each time. This will be discussed in section 3.

3. DEPLETION OF A CFV FUEL ASSEMBLY

The CFV is a core concept that presents strong axial heterogeneities. In this section, the algorithm described in Sec. 2 is applied to produce burnup parametrized 33 group homogenized cross sections for a fuel assembly representative of a CFV core. Such cross sections are then used in a fuel depletion calculation. The APOLLO3® code which is being developed at CEA in France is used. Results are compared to reference Monte Carlo depletion calculations. Some comparisons with standard 2D calculations, which constitute the previous methodology used at CEA to get a fuel assembly cross sections, are also provided.

3.1. Description of the Benchmark

The benchmark, whose geometry is depicted in Fig. 2, has already been introduced in reference [6]. We recall that C1 stands for fissile (U,Pu)O_2 material, FCA for fertile depleted UO_2 media and PLN, PNS, SVE are French acronyms for sodium plenum, axial B_4C neutronic protection and expansion tank (container for gaseous fission products) respectively. Some other internal structures do not appear in the figure to avoid burdening it.

In this study, the depletion duration is set to 1080 days and the assembly power $P = 5.4$ MW is kept constant during this time.

The axial partition of the domain chosen for the 2D/1D algorithm follows the axial layout of the assembly resulting in thirteen 2D layers. In particular, this division leads to five distinct depleting material (two C1 and three FCA, one of which do not appear in Fig. 2 because it is an isolated UO_2 pellet located at the top of the upper C1 zone). Even though this partition is probably inadequate to accurately model the axial concentration gradients, this might not be so troublesome as long as the 2D/1D algorithm is only used to produce burnup parametrized cross sections. A finer axial mesh will be used in the core calculations.

This partition being defined, the 2D/1D depleting equations are solved using a 1968 group cross section library processed from the JEFF-3.1.1 evaluation. The decay chain includes 18 heavy nuclides and 126 fission products [9]. Eqs. (2a) and (2b) are solved respectively with TDT and IDT characteristics solvers of APOLLO3®. Eq. (1b) is solved with the MENDEL [10] depletion solver. To ensure a converged solution, a relatively high number of time steps is chosen leading to 17 points of tabulation for the homogenized cross sections library.

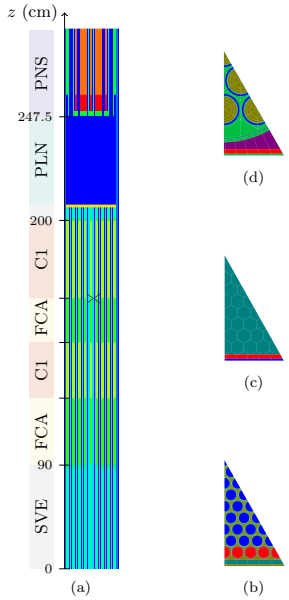

Figure 2. ASTRID internal fuel assembly: (a) axial layout, (b) fuel pins mesh (1/12$^{\text{th}}$), (c) sodium plenum mesh, (d) axial protection mesh

At the end of the 2D/1D depletion calculations, we obtain an effective cross section library parametrized with local burnups (or fluence). Using this library, the depletion calculation is repeated in a "core environment" featuring a simplified version of the assembly in which radial heterogeneities are homogenized. The number of energy groups is also reduced from 1968 to 33. Taking advantage of the simplicity of the model, a fine axial mesh (5 cm) is used to distinguish depleting materials. At this stage, the MINARET S_N solver of APOLLO3® ("core solver") is used together with MENDEL.

Results are compared to Monte Carlo calculations performed with a validated version of the TRIPOLI4® code coupled to the MENDEL depletion solver [11]. They feature the heterogeneous 3D geometry of the fuel assembly and a continuous energy description. A fine time mesh (10 time steps), a second order time scheme and the simulation of 24.10^6 particles per time step ensure an acceptable convergence of the results. In the following, they will be trusted as reference values.

3.2. Numerical Results

The numerical results presented in this section include evolution of the assembly reactivity and isotopic concentrations. Reactivity differences are computed as $\Delta\rho = 10^5\,(1/k_{\mathrm{T4}} - 1/k_{\mathrm{AP3}})$ where k is the multiplication factor handled by the code. We also insist on the fact that APOLLO3® results always stand for results of the "core environment" featuring 33 group homogenized cross sections (i.e. the 2D/1D algorithm is only used to produce cross sections even though it also handles good results).

Fig. 3 presents results for the reactivity loss which is evaluated to -3180 pcm (i.e. ≈ 3 pcm/day). The reactivity difference between APOLLO3® and the reference results clearly shows that 2D/1D cross sections improve the calculation accuracy compared to the standard 2D methodology previously used at CEA. More precisely, the latter presents a 300 pcm difference at $t = 0$ while all 2D/1D results are within a 50 pcm range from reference results. In addition, the evolution of the reactivity difference follows a monotonous pattern with 2D/1D cross sections meanwhile for 2D results the behavior is more irregular.

Benefits of the burnup parametrization of cross sections are less impressive but they show that a 50 pcm extra accuracy can be achieved when the impact of the flux dependency on time is taken into account to produce cross sections. If the transverse leakage splitting correction (TLS) of section 2.3 is applied, all comparisons between APOLLO3® and TRIPOLI4® agree within the statistical 2σ error bar.

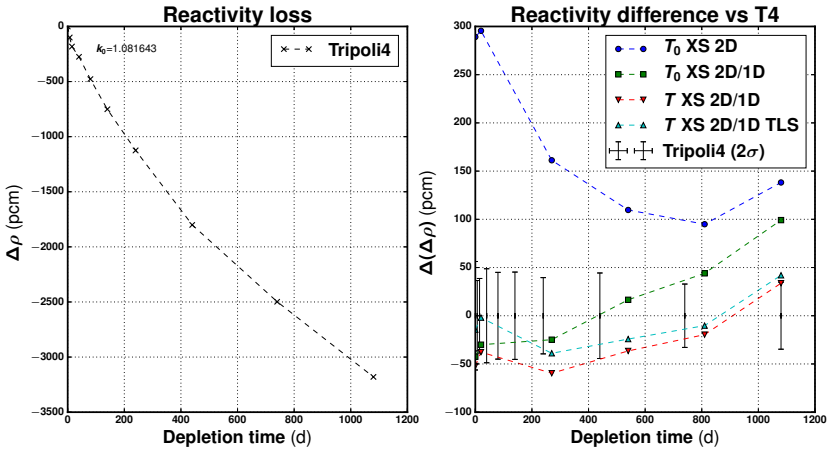

Figure 3. Reactivity loss for fuel assembly depletion (left) and reactivity discrepancy with 2D or 2D/1D cross sections (right). Note: T_0 stands for time-independent cross sections and T for burnup parametrized XS

Fig. 4 now shows how some calculation time can be saved on the resolution of the 2D/1D equations. The impact of the number of tabulated points (i.e. time steps) is evaluated showing that the difference between a cross section library that contains seventeen tabulated burnup points and another one that only contains two such points is less than 20 pcm. In other words, no intermediate calculations are in fact required but most of the effect can be catch with only two transport calculations performed at the initial and final stages of the depletion. Furthermore, Fig 4 also shows that the re-evaluation of non depleting planes (i.e. structures such as the sodium plenum or the neutronic protections) is not necessary. In fact, we observe no difference with the case in which Eq. (2a) is solved for all planes including those ones.

All in one, those results mean that the generation of the cross section library only requires one full 2D/1D transport calculation at $t = 0$, a single isotopic depletion calculation over the full time range and a second "partial" 2D/1D calculation in which Eq. (2a) is not solved for structure planes.

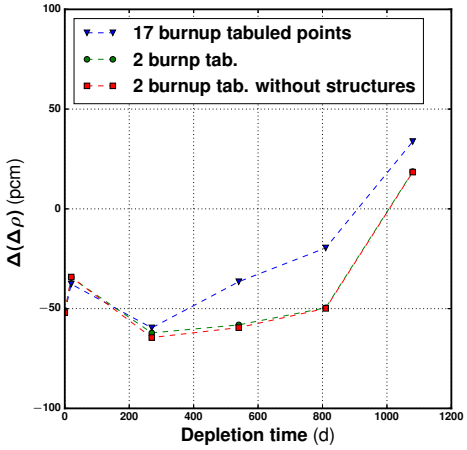

Figure 4. Reactivity discrepancy with 2D/1D cross sections: influence of the number of tabulated burnup points in the cross section library

Finally, Fig. 5 and Tab. I show the concentration results for a selected choice of isotopes including heavy nuclides and fission products. TRIPOLI4® values are presented together with their relative statistical uncertainty (σ/N in percentage) and the relative concentration discrepancy for APOLLO3® results is computed as $\Delta_r = 100\,(N_{\text{AP3}}/N_{\text{T4}} - 1)$.

Tab. I shows that the final concentrations of actinides (Pu239 and Np237) and fission products (Cs133) are well predicted when the 2D/1D method is used to produce the effective cross sections. Most discrepancies are below 1% except in the upper fertile zone (FCA) for which differences can reach a few % (with both 2D and 2D/1D methods). Further investigation is required to understand why such values are found in this zone. On the other hand, we observe that the standard 2D method systematically underestimates the concentration values in fertile layers and especially at the bottom of the assembly. In particular, a 9% discrepancy is found for the concentrations of Cs133 and Np237 in the lower fertile blanket.

	N $(1 \pm 100 * \sigma/N)$ (at/barn/cm)	Δ_r (%) 2D	2D/1D		N $(1 \pm 100 * \sigma/N)$ (at/barn/cm)	Δ_r (%) 2D	2D/1D	
Pu239	1.1E-03 (1 ± 0.05)	-2.64	-5.90	Upper FCA	3.3E-05 (1 ± 0.09)	-3.01	-4.43	Cs133
	1.4E-02 (1 ± 0.006)	+0.06	+0.20	Upper C1	8.9E-04 (1 ± 0.03)	+0.81	-0.69	
	4.6E-03 (1 ± 0.02)	+1.17	-0.28	Medium FCA	1.3E-04 (1 ± 0.04)	-3.2	+0.08	
	1.0E-02 (1 ± 0.006)	+0.18	+0.05	Lower C1	4.6E-04 (1 ± 0.05)	-2.2	-0.54	
	3.2E-03 (1 ± 0.06)	-1.67	-0.39	Lower FCA	3.9E-05 (1 ± 0.10)	-9.1	-0.81	
Np237	4.4E-06 (1 ± 0.37)	-2.63	+1.40	Upper FCA				
	4.7E-05 (1 ± 0.18)	+0.64	+0.56	Upper C1				
	1.7E-05 (1 ± 0.33)	-4.41	+1.13	Medium FCA				
	2.6E-05 (1 ± 0.26)	-1.48	+0.72	Lower C1				
	7.0E-06 (1 ± 0.56)	-8.93	-1.03	Lower FCA				

Table I. Pu239, Np237 and Cs133 concentrations at end of depletion ($t = 1080$ days)

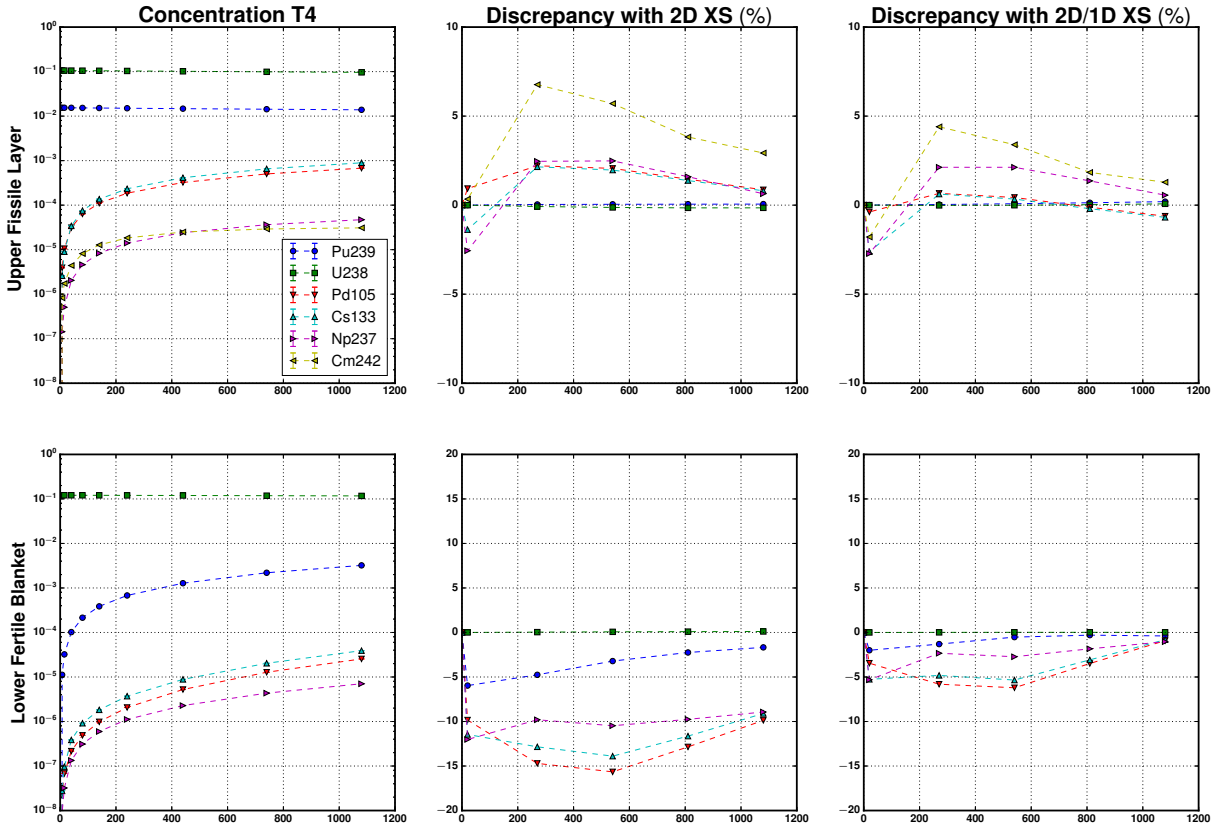

Figure 5. Evolution of isotopic concentrations (left) and relative discrepancy with 2D (center) or 2D/1D (right) cross sections for upper fissile zone and lower fertile blanket

Those results are confirmed by Fig. 5 that presents how the concentrations and discrepancies evolve with time. Additional data for U238, Pd195 and Cm242 are also given. The same conclusions are inferred being the 2D/1D method more precise than standard 2D calculations compared to Monte Carlo results.

4. CONCLUSIONS

This paper presents an algorithm based upon a 2D/1D method to consistently produce time-dependent effective cross sections for SFR depletion calculations. The algorithm is applied to a radially reflected 3D CFV fuel assembly.

The method couples 2D and 1D flux solvers to solve the 3D neutron transport equation and a depletion solver to solve the Bateman equations. Few groups homogenized cross sections are produced at distinct burnup steps and used in a core calculation featuring a simple model of the assembly.

Good performances are found against reference Monte Carlo simulations both for the evolution of the reactivity and isotopic compositions. On the contrary, it is shown than cross sections produced with standard 2D models present a bias on the spatial distribution of isotopic concentrations and larger discrepancies on reactivity. Finally, the number of points of tabulation needed for the construction of the cross sections library can be optimized to decrease the overall calculation time.

The method has recently been used in a realistic full core calculation in which radial heterogeneities are correctly taken into account (the CFV core presents two enrichment zones for fuel assemblies and a reflector). Encouraging results have been found and shall be presented in a near future.

ACKNOWLEDGEMENTS

The authors acknowledge the CEA of Cadarache for funding this work, FRAMATOME and EDF for their long term support and the APOLLO3® development team for the provided support.

REFERENCES

[1] A. Hébert. *Applied Reactor Physics*. Presses internationales Polytechnique, 2009.

[2] H. Bateman. Solution of a System of Differential Equations Occurring in the Theory of Radioactive Transformations. Proc. Cambridge Philos. Soc., 15:423–427, Cambridge, 1910.

[3] N. Z. Cho, G. S. Lee, and C. J. Park. A Fusion Technique of 2D/1D Methods for Three-Dimensional Whole-Core Transport Calculations. *Proc. Korean Nuclear Society*, 2002.

[4] D. Schneider, F. Dolci, F. Gabriel, J. Palau, M. Guillo, and B. Pothet. APOLLO3: CEA/DEN Deterministic Multi-Purpose Code for Reactor Physics Analysis. In *Proc. Int. Conf. PHYSOR 2016 - Unifying Theory and Experiments in the 21st Century*, Sun Valley, Idaho, United States, 2016. American Nuclear Society.

[5] T. Beck, V. Blanc, J.-M. Escleine, D. Haubensack, M. Pelletier, M. Phelip, B. Perrin, and C. Venard. Conceptual Design of ASTRID Fuel Sub-assemblies. *Nuclear Engineering and Design*, 315:51–60, 2017.

[6] B. Faure, P. Archier, J.-F. Vidal, and L. Buiron. A 2D/1D Algorithm for Effective Cross-Section Generation in Fast Reactor Neutronic Transport Calculations. *Nuclear Science and Engineering*, *online*, 2018.

[7] B. Collins, S. Stimpson, B. W. Kelley, M. T. Young, B. Kochunas, A. Graham, E. W. Larsen, T. Downar, and A. Godfrey. Stability and Accuracy of 3D Neutron Transport Simulations using the 2D/1D Method in MPACT. *Journal of Computational Physics*, 326:612–628, 2016.

[8] J.-F. Vidal, P. Archier, B. Faure, V. Jouault, J.-M. Palau, V. Pascal, G. Rimpault, F. Auffret, L. Graziano, E. Masiello, et al. APOLLO3 Homogenization Techniques for Transport Core Calculations - Application to the ASTRID CFV Core. *Nuclear Engineering and Technology*, 49:7:1379-1387, 2017.

[9] P. Archier, S. Domanico, J. Palau, and G. Truchet. Validation of a Multi-Purpose Depletion Chain for Burnup Calculations through TRIPOLI-4 Calculations and IFP Perturbation Method. *PHYSOR. Sun Valley, USA*, 2016.

[10] S. Lahaye, P. Bellier, H. Mao, A. Tsilanizara, and Y. Kawamoto. First Verification and Validation Steps of MENDEL Release 1.0 Cycle code system. *PHYSOR 2014*, 2014.

[11] Y.-K. Lee, E. Brun, and X. Alexandre. SFR Whole Core Burnup Calculations with TRIPOLI-4 Monte Carlo Code. In *Proc. Int. Conf. PHYSOR 2014 - The Role of Reactor Physics Toward a Sustainable Future*. American Nuclear Society, 2014.